ELSEVIER

Polymer 43 (2002) 2897–2908

polymer

www.elsevier.com/locate/polymer

Influence of chain microstructure on the conformational behavior of ethylene-1-olefin copolymers. Impact of the comonomeric mole content and the catalytic inversion ratio

Tarek M. Madkour[a,1,*], Bart Goderis[a], Vincent B.F. Mathot[a,b], Harry Reynaers[a]

[a]*Laboratorium voor Macromoleculaire Structuurchemie, Departement Scheikunde, Katholieke Universiteit Leuven, Celestijnenlaan 200F, B-3001 Heverlee, Belgium*

[b]*DSM Research, P.O. Box 18, 6160 MD Geleen, The Netherlands*

Received 5 December 2001; received in revised form 21 December 2001; accepted 21 December 2001

Abstract

The rotational isomeric state model was employed to provide a better understanding of the role of chain microstructure on the conformational behavior of homogeneous ethylene-1-olefin copolymers. The chain microstructure was assembled in accordance with the copolymerization theory using a set of conditional probabilities in direct relation to the reactivity ratios and the feed compositions of the comonomers. The catalytic inversion influence on the tacticity of the polymeric microstructure was also taken into account by considering the replication probability during the Monte Carlo simulation. Statistical weight factors of the rotational isomeric states were evaluated using molecular dynamics runs of the various homopolymers according to the earlier work of Mattice et al. Probability distribution surfaces constructed by the integration of the molecular dynamics trajectories of sufficient length to sample all of the conformational space indicated the increase of the probability of $g^{\pm}t$ joint states at the expense of $g^{\pm}g^{\pm}$ pairs with the increase in the side chain length of the 1-olefin comonomers. It was also indicated that this behavior had a maximum around poly(1-butene)/poly(1-hexene) with an apparent reversal in case of poly(1-octene) due to the side chain crowding, which forces the chain to favor more of the $g^{\pm}g^{\pm}$ joint states. The characteristic ratios calculated for the copolymers on the basis of the rotational isomeric state model also indicated the increased extension of the polymer backbone with the increase in the side chain length. The lower characteristic ratio calculated for the octene polymers may, in fact, explain the experimental observation that poly(1-octene) has a lower melting point than those of other poly(1-olefin)s of shorter side chains. A complete account of the role of tacticity on the characteristic ratio and the radial distribution function is also given.

Keywords: Ethylene-1-olefin; Copolymers; Comonomers

1. Introduction

The emergence of single site catalysts such as Vanadium-based catalysts or constrained geometry catalysts has led to new development of ethylene copolymers such as the ethylene-1-olefin series with specific chain microstructures [1]. The main characteristic of these copolymers is that they are 'homogeneous' copolymers in the sense that they can be described with a single set of reactivity values corresponding to a single active catalyst site. Moreover, chains of homogeneous copolymers will display no differences in comonomer incorporation other than differences relating to the statistical fluctuations [2]. This is because the set of reactivity ratios that defines the polymerization process can be described by a first-order Markovian process. Since the comonomer units add to the growing chain either in isolation or in very short sequences, they hinder the crystallization of the longer ethylene sequences during processing. This implies that the exact distribution of the comonomer units along the chain determines the crystallizability of that chain and influences the morphology and the ultimate properties of the final copolymer. Mathot et al. [3,4] developed a special model in order to determine the chain microstructure of these copolymers on the basis of ^{13}C-NMR spectra. A special model was needed since the (promoted) catalytic system used in the preparation of these materials consisted of an aluminum alkyl combined with a Vanadium component, giving rise to incorporation of 'normal' and 'inverted' comonomers. The use of this model led to the elucidation of the sets of reactivity ratios as related to the chain propagation probabilities and the information

* Corresponding author.

[1] On a leave of absence from the Department of Chemistry, Helwan University, Ain-Helwan, Cairo 11795, Egypt.

0032-3861/02/$ - see front matter
PII: S0032-3861(02)00085-X

regarding the sequence lengths and sequence length distributions of the copolymers with side chains of various lengths.

The amount and exact distribution of the comonomer units along the chain determines the length of the ethylene sequences and hence the intrinsic crystallizability of the polymer chains. According to classical views, polymeric chains change their melt conformation upon crystallization from a disordered coil into a conformation that is suitable for attachment to a growing crystal [5,6]. There is, however, increasing evidence for an ordered melt state prior to crystallization [7–9] but at present, there is no way to generalize the chain conformational behavior. This, particularly, holds for ethylene-1-olefin copolymers since, in addition to the intrinsic chain characteristics such as the molar mass and degree and type of branching, chain conformational behavior is most likely being influenced by the interaction with neighboring chains. Furthermore, one would expect aliphatic polyolefins to be miscible, since the enthalpy of mixing is virtually zero and there are no specific interactions. This, however, is not always the case. Recently, packing constraints were recognized as a potential reason for demixing since they may alter interactions (enthalpy) or give rise to non-local excess entropy of mixing contributions [10–12]. Clearly, in the present case of ethylene-1-olefin copolymers and most likely in general, a link between chain microstructure and crystallization behavior or miscibility cannot be made without considering melt chain conformational behavior [13]. Furthermore, crystallization and miscibility behavior in turn provide a sample with a given morphology and consequently with a set of characteristic properties such as the stiffness, ductility, tear strength, clarity and softening temperature [14,15]. Unlike long chain branching, short chain branching (as e.g. obtained by the copolymerization of ethylene with 1-olefins) does not influence the melt rheology of the polymers directly, but rather it influences the mass–size relationship [16,17].

To investigate the interesting characteristics of these polymers, Flory [18–20] have applied the rotational isomeric state (RIS) concept conceived by Volkenstein [21] and Birshtein and Ptitsyn [22] to evaluate the conformational behavior and unperturbed dimensions of polydiene and polyolefins in direct relation to the configuration-dependent properties such as the characteristic ratio, the mass–size relationship and the specific volume. The majority of the RIS predictions have been verified by experiment for polyethylene [23], polybutadiene [24], polyisoprene [25], polyisobutylene [26] and ethylene–propylene copolymers [27]. According to Mattice [28], the presence of the longer side chains in a polymer affects its end-to-end distance separation and subsequently its characteristic ratio since the interactions of the side groups with the main chain will depend on the conformations they and the main chain may adopt. Flory and co-workers [18,20,29] have recognized the difficulty of accommodating an articulated side chain if the main chain bonds flanking its point of attachment to the backbone both occupy *trans* states. They, therefore, incorporated a distinctive factor in the statistical weight matrices specially to account for the low probability of occurrence for the *tt* sequence while treating only the first- and second-order interactions. Mattice and Suter have indicated [30], however, that when the side chains, or the density of their attachments to the main chain, produce numerous short-range interactions that include important interactions higher than second-order, methods based on specific enumeration of all of the relevant short-range interactions may be necessary. The numeric values of the elements in the statistical weight matrices may, therefore, be determined by integration of the conformational energy surface as was done for poly(4-methyl-1-pentene) and poly[(S)-methyl-1-hexene] by Wittwer and Suter [31] or by integration of a molecular dynamics (MD) trajectory of sufficient length to sample all of the conformational space, as was done for poly(dialkyl siloxanes) by Mattice et al. [32]. It was reported [32–34] that MD trajectories of sufficient duration to sample all conformational space are shown to yield information on (i) the types of isomeric states accessible to backbone bonds, (ii) their probability distribution, and (iii) the mechanism and rate of transitions between them. The formulation of the statistical weight matrices of the rotational isomeric state approximation [18] via quantitative analysis of MD trajectories has been outlined for chains of bonds with symmetric 3-fold rotational potentials [35]. The major advantage following this approach over the classical one of considering the usual first- and second-order interactions alone is the successful assessment of the probability distribution of the isomeric states for chains in which the interactions between the successive bulky side groups and the main chain dominate the behavior of the chain.

2. Theoretical methodology

2.1. Chain microstructure assemblage

In the study of chemical copolymers, the first requirement is the generation, or simulation, of chains having chemical and stereochemical structures, which can be related to the nature of the comonomers and the conditions under which the copolymerization was carried out. The distribution of the monomer units along the chain is controlled by the conditional probabilities P_{ij} that a chain ending in monomer type i will add a unit of type j. In the case of binary copolymers, these probabilities are P_{11}, P_{22}, $P_{12} = 1 - P_{11}$ and $P_{21} = 1 - P_{22}$, and according to copolymerization theory, are specified by Ref. [27]:

$$P_{11} = r_1F_1/(r_1F_1 + F_2) \tag{1}$$

$$P_{22} = r_2F_2/(r_2F_2 + F_1) \tag{2}$$

In these equations, r_1 and r_2 are reactivity ratios and are

Table 1
Reactivity ratios for the various simulated systems [1–4,48,49]

Simulated copolymers	r_1	r_2	$r_1 r_2$
Ethylene/propylene	16.374	0.032	0.53
Ethylene/1-butene	19.136	0.027	0.51
Ethylene/1-hexene	21.898	0.021	0.46
Ethylene/1-octene	24.661	0.017	0.41

defined by:

$$r_1 = k_{11}/k_{12} \tag{3}$$

$$r_2 = k_{22}/k_{21} \tag{4}$$

where k_{ij} is the rate constant for the addition of monomer of type j to a growing chain end of type i. r_1 and r_2 calculated on the basis of NMR data interpolation are given in Table 1. F_1 and $F_2 = 1 - F_1$ are the mole fractions of monomers M_1 and M_2, respectively, in the monomer mixture undergoing copolymerization. For very long chains prepared in a system of constant composition, the fraction f_1 of units of type 1 in the chain will equal to the value of the probability P_1 that a monomer unit being incorporated into a growing chain is type 1; this quantity is given by Refs. [27,36]:

$$P_1 = \left(r_1 F_1^2 + F_1 F_2\right)/\left(r_1^2 F_1^2 + 2F_1 F_2 + r_2 F_2^2\right) \tag{5}$$

The above set of equations indicates that specifications of f_1 and the product $r_1 r_2$ determines the values of P_{11} and P_{22} required to give a chain having the desired characteristics. Values of P_{11} and P_{22} thus calculated may be used in conjunction with a set of X random numbers ranging in magnitude from 0 to 1 to simulate [37] using Monte Carlo methods a copolymerization leading to a chain of X monomer units. The magnitude of the first number relative to P_1 is used to specify the chemical nature, or type, of the first unit in the chain; subsequent numbers are compared with either P_{11} or P_{22}, depending on the nature of the preceding unit, to determine the type of monomer used in subsequent additions. The studied systems were simulated as to resemble copolymers synthesized under conditions that favor both intramolecular and intermolecular uniformity in the comonomer incorporation statistics, i.e. homogeneous copolymers [1,2].

The generation of the stereochemical structures of sequences of asymmetric units may also be carried out using the Monte Carlo technique on other sets of random numbers [27]. The locations and lengths of the sequences of asymmetric units are specified by the Monte Carlo generation of the chemical structure. For each such sequence, the magnitude of the first number generated is compared with 0.5 in order to specify the atomic configuration of the first unit. Thereafter, occurrence of a number less than the chosen value of the replication probability P_r (the probability that the stereochemical configuration of the asymmetric center –CHR-corresponds to that of its predecessor in the chain) is taken to specify an isotactic placement (replication), and a number greater than P_r, syndiotactic placement (inversion). For very long chains, the fraction f_r of isotactic placement in the chain will be equal to the value chosen for P_r.

2.2. Configuration partition function

The rotational isomeric state model for vinyl chains has been extensively discussed [18,26,27], as has its specific application to the calculation of the random coil, unperturbed dimensions $\langle r^2 \rangle_0$ of polyolefins such as polyethylene chains [18,38] and polypropylene chains of various stereochemical compositions [18,29]. Following these analyses, we adopt the rotational states: *trans* (t), *gauche*$^+$ (g^+), and *gauche*$^-$ (g^-) for the chain skeletal bond, such as bonds $i-3$ to $i+2$ of Fig. 1. For the purpose of calculating configuration-dependent properties, such statistical weights are used to construct statistical weight matrices $\mathbf{U}_i$. In such matrices, rows are associated with rotational states about bond $i-1$ and columns, with states about bond i; both rows and columns are indexed in the order t, g^+, g^-. For CH_2–CH_2–CH_2 (ethylene) bond pairs, the statistical weight matrix is designated $\mathbf{U}_e$ and has the form:

$$\mathbf{U}_e = \begin{bmatrix} 1 & \tau/\eta & \tau/\eta \\ 1 & \tau/\eta & \tau\omega/\eta \\ 1 & \tau\omega/\eta & \tau/\eta \end{bmatrix} \tag{6}$$

For a pair of bonds meeting at a –CHR-group, the atomic configuration of the group must be specified. Adoption of the arbitrary d, l convention, Fig. 1, previously employed [27,29] yields, for the statistical weight matrix characterizing bonds meeting at a C atom of d configuration,

$$\mathbf{U}_d = \begin{bmatrix} \eta & 1 & \tau \\ \eta & 1 & \tau\omega \\ \eta & \omega & \tau \end{bmatrix} \tag{7}$$

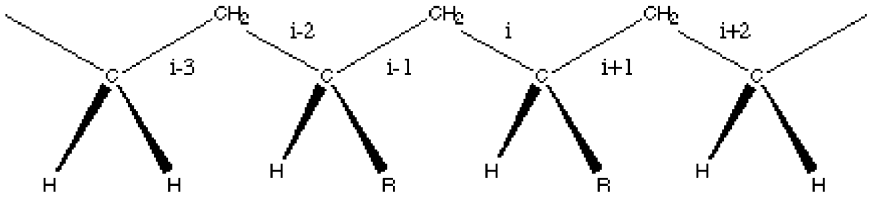

Fig. 1. The planar, all-*trans* conformation of a portion of ethylene-1-olefin chain. The 1-olefin sequence shown constitutes an isotactic (*dd*) dyad. The lines of increasing and decreasing thickness represent bonds extending toward and away from the reader, respectively.

By symmetry, the matrix $\mathbf{U}_l$ associated with a C atom of l configuration is obtained by simple interchange [18] of both the second and third rows and the second and third columns of $\mathbf{U}_d$. In the case of pairs of bonds separating two –CHR-groups, the configuration of both groups must be specified. The statistical weight matrices for the dyads *dd* and *dl* are given by

$$\mathbf{U}_{dd} = \begin{bmatrix} \eta\omega & \tau\omega & 1 \\ \eta & \tau\omega & \omega \\ \eta\omega & \tau\omega^2 & \omega \end{bmatrix} \tag{8}$$

$$\mathbf{U}_{dl} = \begin{bmatrix} \eta & \omega & \tau\omega \\ \eta\omega & 1 & \tau\omega \\ \eta\omega & \omega & \tau\omega^2 \end{bmatrix} \tag{9}$$

The matrices $\mathbf{U}_{ll}$ and $\mathbf{U}_{ld}$ may be obtained from $\mathbf{U}_{dd}$ and $\mathbf{U}_{dl}$, respectively, by the interchanges of rows and columns described above. Bond pairs CHR–CH_2–CH_2 are characterized by the matrices $\mathbf{U}_{de}$ and $\mathbf{U}_{le}$ where

$$\mathbf{U}_{de} = \begin{bmatrix} \eta/\tau & \omega & 1 \\ \eta/\tau & 1 & \omega \\ \eta/\tau & \omega & \omega \end{bmatrix} \tag{10}$$

and $\mathbf{U}_{le}$ is related to $\mathbf{U}_{de}$ simply by the symmetry operations already described. Similarly, the matrices $\mathbf{U}_{ed}$ and $\mathbf{U}_{el}$ are associated with bond pairs CH_2–CH_2–CHR, with

$$\mathbf{U}_{ed} = \begin{bmatrix} \eta & \tau & 1 \\ \eta & \tau\omega & \omega \\ \eta\omega & \tau\omega & 1 \end{bmatrix} \tag{11}$$

and $\mathbf{U}_{el}$ having the usual relationship to $\mathbf{U}_{ed}$.

Using the above statistical weight matrices, the configuration partition function Z for an ethylene-1-olefin chain of n bonds, or $X = n/2$ repeat units, can be written as [18]

$$Z = \mathbf{J}^* \left[\prod_{i=2}^{n-1} \mathbf{U}_i \right] \mathbf{J} \tag{12}$$

where $\mathbf{J}^* = [1\ 0\ 0]$ and $\mathbf{J}$ is the transpose of [1 1 1]. Calculation of mean-square unperturbed dimensions from skeletal bond vectors $\mathbf{l}$ requires construction of Cartesian coordinates systems about each bond in the chain backbone. If the x-axis is taken along bond i, and the positive y-axis is taken in the plane determined by bonds i and $i-1$ so as to make an acute angle with bond $i-1$, then the matrix $\mathbf{T}_i$ which transforms a vector in coordinate system $i+1$ into that of system i is [18]

$$\mathbf{T}_i = \begin{bmatrix} \cos\theta_i & \sin\theta_i & 0 \\ \sin\theta_i\cos\phi_i & -\cos\theta_i\cos\phi_i & \sin\phi_i \\ \sin\theta_i\sin\phi_i & -\cos\theta_i\sin\phi_i & -\cos\phi_i \end{bmatrix} \tag{13}$$

where θ is the bond angle supplement. The rotational angle ϕ is defined relative to a value of 0 for the *trans* state, with positive value corresponding to right-handed rotations, as described elsewhere [18,26,27,39]. The characteristic ratio is then given by

$$\langle r^2\rangle_0/nl^2 = 2(Znl^2)^{-1}\mathbf{I}^*\mathbf{G}_1\left[\prod_{i=2}^{n-1}\mathbf{G}_i\right]\mathbf{G}_n\mathbf{I} \tag{14}$$

where $\mathbf{I}^*$ is the row vector consisting of a single unity followed by 14 zeros, and $\mathbf{I}$ is the column vector consisting of 12 zeros followed by three unities.

As described above, the $\mathbf{U}_i$ and $\mathbf{G}_i$ depend in general on the chemical and stereochemical natures of both the monomer unit in which bond i is located and its predecessor along the chain. The precise sequences of **U**s and **G**s appearing in Eqs. (12) and (14) are specified by Monte Carlo methods, as described elsewhere [40].

2.3. Probability distribution surfaces

The statistical weights or the statistical weight matrices could be computed for polypropylene (PP), poly(1-butene) (PB), poly(1-hexene) (PH) and poly(1-octene) (PO) following the method of Mattice et al. [32] utilizing molecular dynamics simulations of polymeric fragments of ten repeat units in vacuum at 473 K using Cerius [2] software package, MSI, and employing the COMPASS forcefield [41]. The duration of the simulations was chosen to be long enough (10 ns) to allow for sufficient sampling of the conformational space. In all cases, the initial conformation, where all the internal backbone bonds are in the *trans* state, was minimized using a conjugate gradient method. The simulation was then performed by using the Verlet algorithm [42] to integrate the equation of motion for all atoms with time increments of 0.5 fs. Hydrogen atoms were included explicitly. Isothermal conditions were maintained by rescaling the instantaneous velocities of the atoms at intervals of 1 ps. From the history of dihedral angles, a wide variety of torsional states was observed to have been visited by the backbone bonds of all the fragments, with substantial fluctuations taking place over time ranges of picoseconds. A closer examination of the time and space distribution of dihedral angles indicated, however, that the torsional motions of the two bonds centered about the carbon atoms bearing the side chains are not independent of each other but occur in a concerted fashion. A systematic analysis of pair correlation between neighboring bonds is made possible by the examination of the probability distribution surfaces constructed as a function of two consecutive bond rotations, Figs. 2–5. Similar 3D plots were previously drawn for polyethylene, polydimethylsiloxane, polyisobutylene and poly(vinyl chloride) [33,43,44].

The basic procedure involves the consideration of the conformational space defined by the complete revolutions of two adjacent bond angles, ϕ_i and ϕ_{i+1}, to divide it into small subspaces (36×36) of dimensions $(\Delta\phi_i, \Delta\phi_{i+1}) = (10°, 10°)$ and to record the overall residence time in each

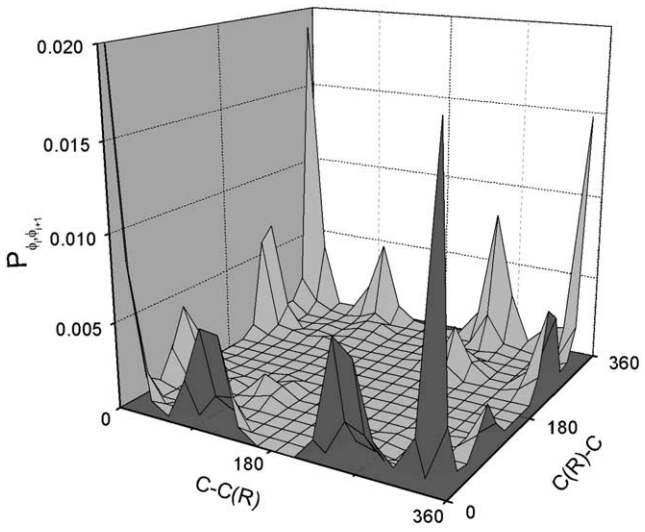

Fig. 2. Probability distribution surface $P(\phi_i, \phi_{i+1})$ for the torsional angles (ϕ_i, ϕ_{i+1}) in polyethylene obtained from MD simulations at 473 K.

subspace. Normalization of the latter yields the probability $P(\phi_i, \phi_{i+1})$ of occurrence of the joint state (ϕ_i, ϕ_{i+1}) representative of a given subspace. Fig. 2 shows the probability distribution surface for polyethylene. In the figure, it is obvious that the most preferred dihedral angle pair correlation is *tt* having the highest probability of occurrence. The dihedral pairs of $tg^{\pm}$ and $g^{\pm}t$ do exist but with less probability of occurrence followed by a small probability for the pairs $g^{\pm}g^{\pm}$ in complete agreement with well known data for polyethylene [18,27]. Figs. 3–5 represent the probability distribution surfaces for the various isotactic, syndiotactic and atactic homopolymers, respectively. In all the figures, (a) refers to PP, (b) refers to PB, (c) refers to PH and (d) refers to PO. Fig. 3 indicates the influence of increasing the side chain length in case of the isotactic homopolymers on the probability of occurrence of a joint state. It is obvious that the increased length of the side chain has increased the probability of the joint states $g^{\pm}t$ on the expense of $g^{\pm}g^{\pm}$ pairs leading, therefore, to an apparent extension of the

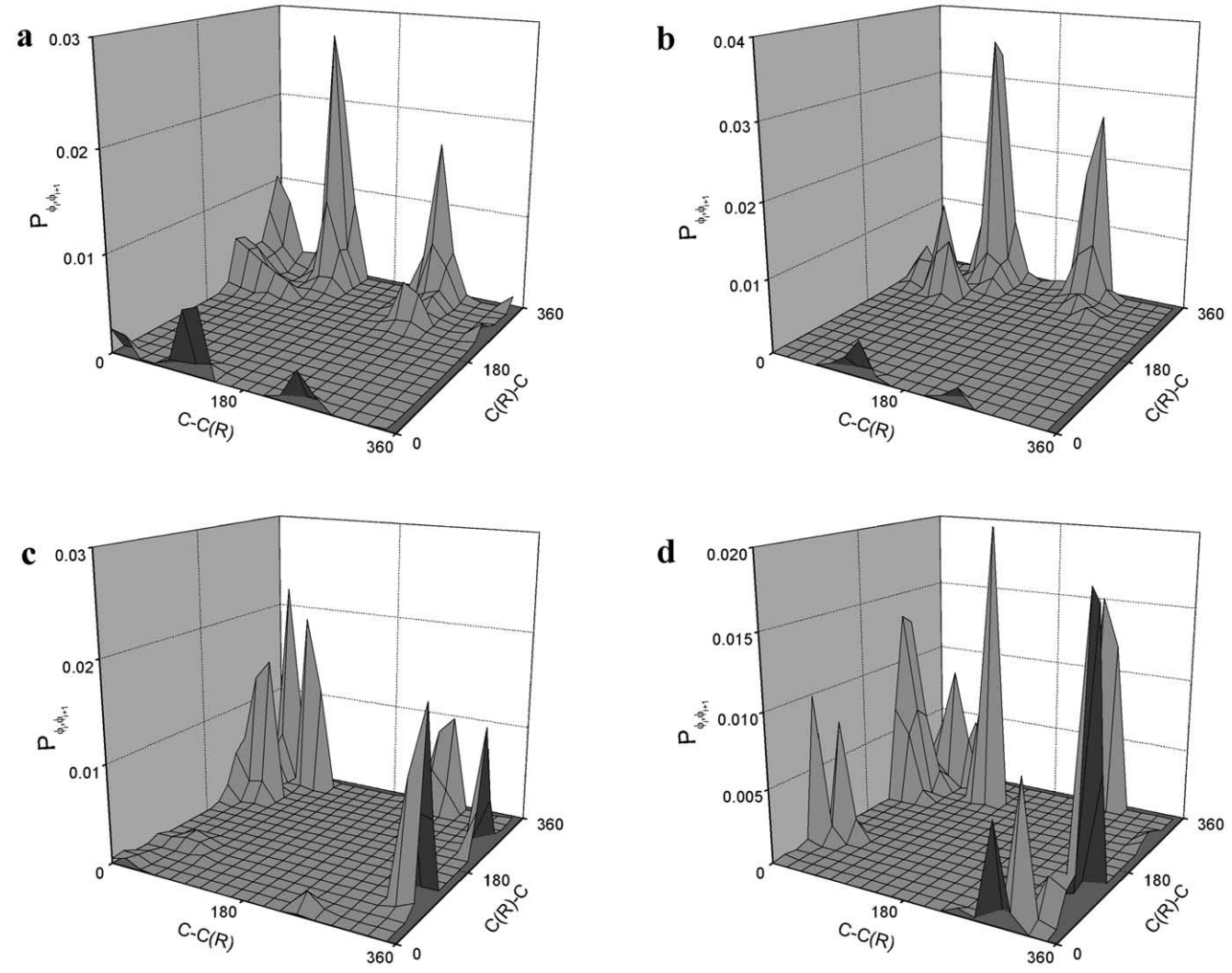

Fig. 3. Probability distribution surfaces $P(\phi_i, \phi_{i+1})$ for the torsional angles (ϕ_i, ϕ_{i+1}) of the pair of bonds centered about the C atom bearing the side chain in isotactic (a) PP, (b) PB, (c) PH, and (d) PO, obtained from MD simulations at 473 K.

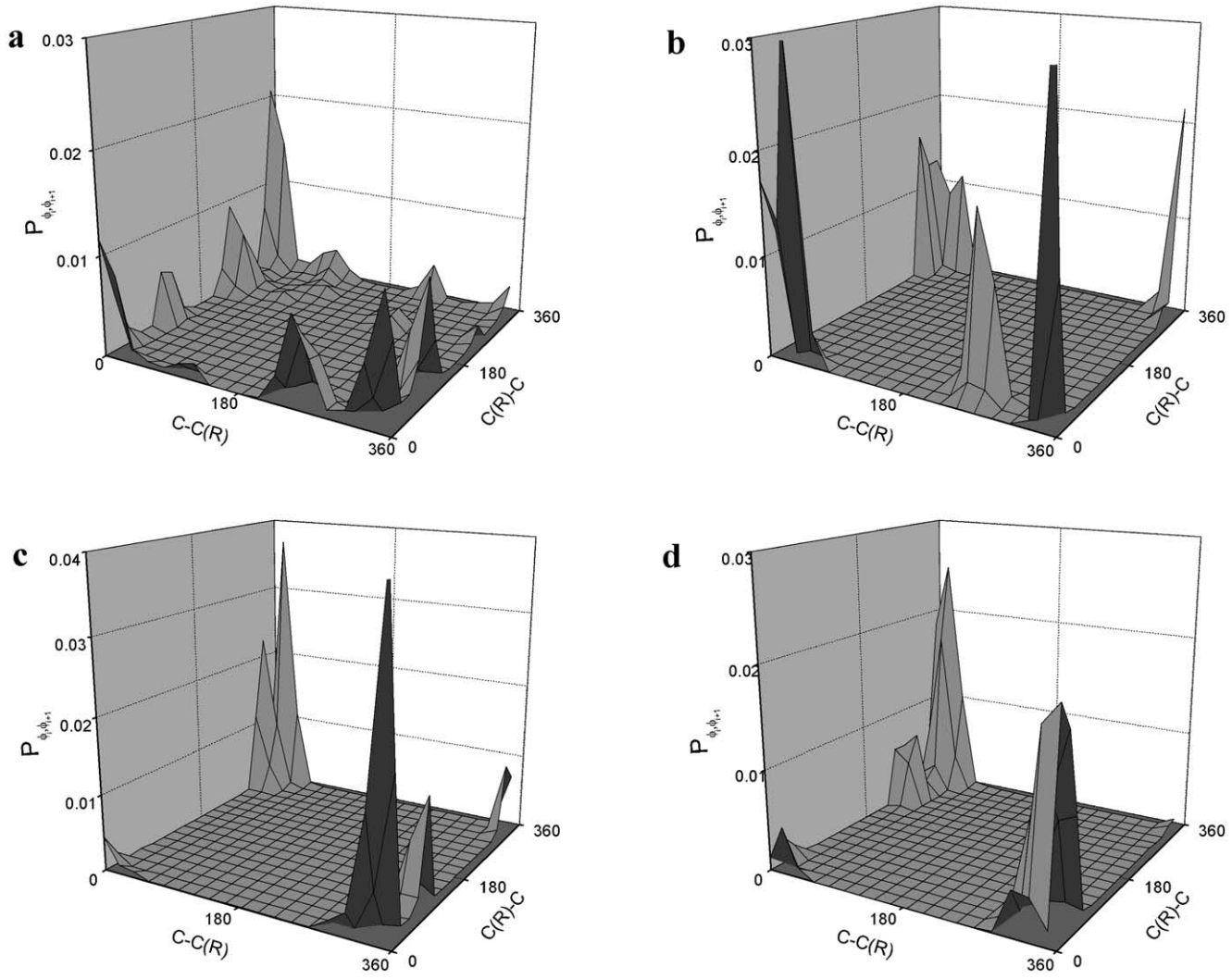

Fig. 4. Probability distribution surfaces $P(\phi_i, \phi_{i+1})$ for the torsional angles (ϕ_i, ϕ_{i+1}) of the pair of bonds centered about the C atom bearing the side chain in syndiotactic (a) PP, (b) PB, (c) PH, and (d) PO, obtained from MD simulations at 473 K.

polymeric chains. A further increase in the side chain length as is the case of PO has actually reversed this effect as evident by its probability distribution surface. This could be illustrated by considering the proximity of the side chains in a polymer with large substituents. The side chains are separated by only two bonds in the main chain between the sites of attachments of the branches, the first atoms in the two successive branches can participate in a second-order interaction. Side chain crowding near the backbone produced by a possible high density of the side chains will exist leading to short range interactions of higher order contribution to the overall configuration partition function [30]. Similar behavior was also obtained for the syndiotactic stereochemical structures, Fig. 4. Interestingly, syndiotactic PO had a better-ordered pair correlation than isotactic PO. This is due to the lessening in the side chain crowding resulting from the configurational placements of the side chains along the two sides of the polymer backbone. The large substituents, all placed on the same side of the backbone, as in the case of isotactic PO, force the main backbone to favor more the *gauche*$^+$ and *gauche*$^-$ dihedral states in order to accommodate the side chain crowding. In the case of syndiotactic PO, the side chains force the polymer chain to assume more of the *trans* torsional angle in order to accommodate the large size of the substituents placed opposite each other along the main backbone. The atactic polymers, Fig. 5, as would be expected, show less order for the pair correlation of the dihedral angles as compared to both the isotactic and syndiotactic polymers, Figs. 3 and 4.

3. Results and discussion

The characteristic ratios $C_n = \langle r^2 \rangle_0 / nl^2$ calculated according to Eq. (14) for the various 1-olefin homopolymers are shown in Figs. 6–8 for the isotactic, syndiotactic and atactic homopolymers, respectively. A gradual increase in C_n was observed for all the different homopolymers with X,

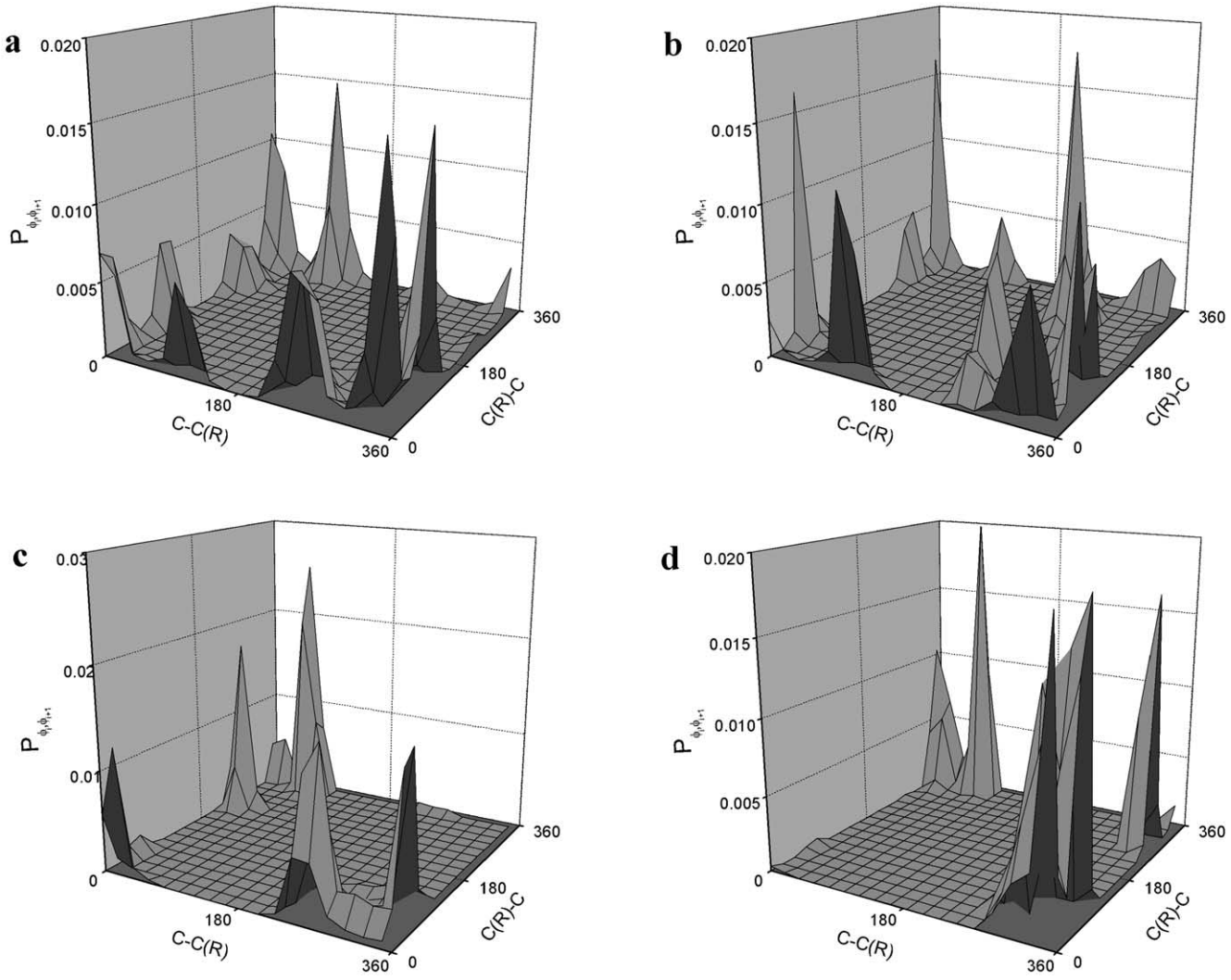

Fig. 5. Probability distribution surfaces $P(\phi_i, \phi_{i+1})$ for the torsional angles (ϕ_i, ϕ_{i+1}) of the pair of bonds centered about the C atom bearing the side chain in atactic (a) PP, (b) PB, (c) PH, and (d) PO, obtained from MD simulations at 473 K.

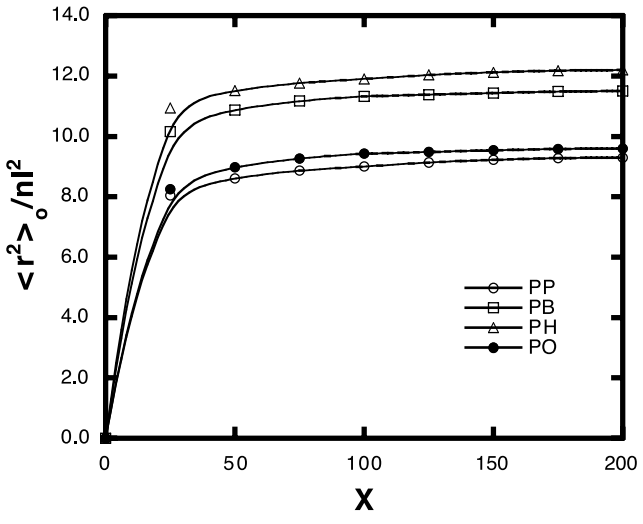

Fig. 6. Characteristic ratio, $C_n = \langle r^2 \rangle_0 / nl^2$, of isotactic PP, PB, PH, and PO as a function of the degree of polymerization, X, calculated at 473 K.

the degree of polymerization, which levels off around $X = 100$ indicating that the characteristic ratio at these levels is very close to its value in the limit of very large X. This is also an indication that the value of 200 units chosen for the degree of polymerization for all the homopolymers and the copolymers studied in this work is sufficiently high and that the behavior of the characteristic ratio at this value is independent of the degree of polymerization and rather dependent on the nature of the chain microstructure of the various polymers. For the isotactic case, Fig. 6 shows the natural increase in C_n with the increase in the side chain length since chains with larger substituent are highly strained and experience stronger repulsive first-order interactions. The observed behavior is consistent with suggestions that persistence length begins to increase owing to an increase in the side group length [10–12]. Interestingly, further increase in the side chain length results in the eventual decrease in the characteristic ratio, as is the case with 1-octene homopolymer. This abnormal result is due to

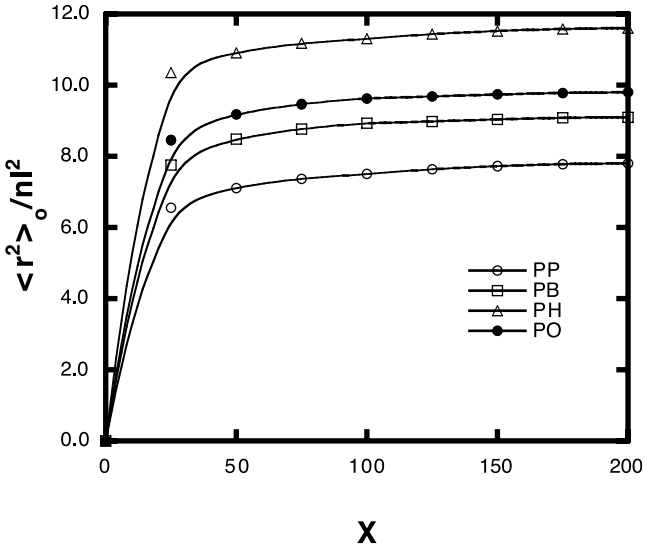

Fig. 7. Characteristic ratio, $C_n = \langle r^2 \rangle_0 / nl^2$, of syndiotactic PP, PB, PH, and PO as a function of the degree of polymerization, X, calculated at 473 K.

the increased frequency for potential overlaps between the long side chains giving rise to third- and higher-order interactions. These side chains mutually exclude each other from otherwise accessible space and the longer the side chain is, the more relevant this space exclusion must be. At such a point, when the side chains are long enough and much more excluded space is therefore necessary, the main backbone chain may have to coil onto itself to allow for the longer side chains to point outwards, giving rise to a much lower values for the unperturbed end-to-end distance and subsequently lower values for the characteristic ratio. This conformational behavior may in fact explain the experimental observation that some sort of transition in the physical properties such as the specific volume or the intrinsic viscosity of poly(1-olefin)s does occur with the inflection point around the poly(1-hexene) and/or poly(1-heptene) [13,14]. Similarly, this may also explain the much lower melting point as well as the obscure melting behavior observed for poly(1-octene) [15–17]. Similar observations could also be obtained for the syndiotactic cases, Fig. 7. The curtailed increase in the characteristic ratio of the syndiotactic polymeric chains with the increase in the side chain length is due to the influence of the syndiotactic placements in obstructing the perpetuation of the preferred helix conformation for the perfect isotactic chain. The physical basis for these results is that the syndiotactic chain is being forced toward the helical conformation represented by $(g^+g^+)(tt)(g^-g^-)(tt)(g^+g^+)(tt)$, etc. Comparison between the results obtained for stereoregular cases, Figs. 6 and 7, and those obtained for the irregular atactic polymer chains, Fig. 8, indicated the sensitivity of the unperturbed dimensions of the polymeric chains to the stereochemical microstructure. In case of the atactic polymer, C_n did increase with the increase in the side chain length, but showed no maximum at PB or PH. In fact, PO had the highest C_n of all studied atactic homopolymers due to the lessening of the side group crowding effect.

The characteristic ratios of the copolymeric microstructures of degree of polymerization of $X = 200$ simulated using Monte Carlo methods as described in Section 2 are shown in Figs. 9–12 for the ethylene copolymers of 1-propylene, 1-butene, 1-hexene and 1-octene, respectively. For all the figures, the characteristic ratios of the isotactic ($P_r = 0.95$), the syndiotactic ($P_r = 0.05$) and the atactic ($P_r = 0.5$) microstructures [27] were all investigated. Chain microstructures were accepted as being representative of the copolymers if the differences between f_1 and P_1 and between f_r and P_r were both less than 0.05; other sequences were discarded. Results obtained are given as a

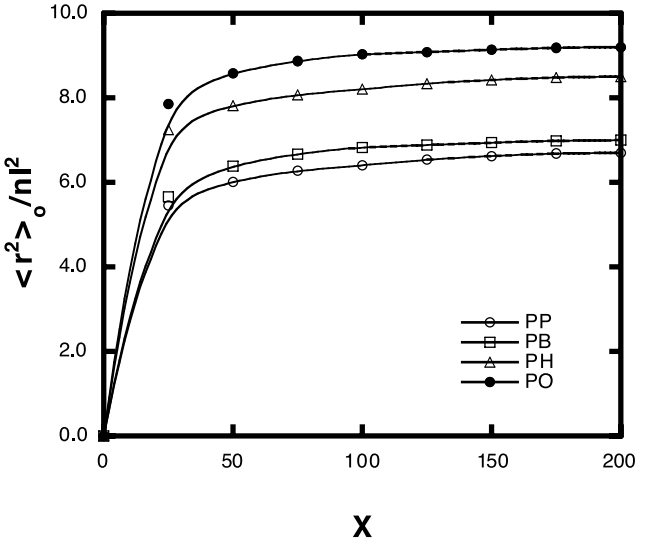

Fig. 8. Characteristic ratio, $C_n = \langle r^2 \rangle_0 / nl^2$, of atactic PP, PB, PH, and PO as a function of the degree of polymerization, X, calculated at 473 K.

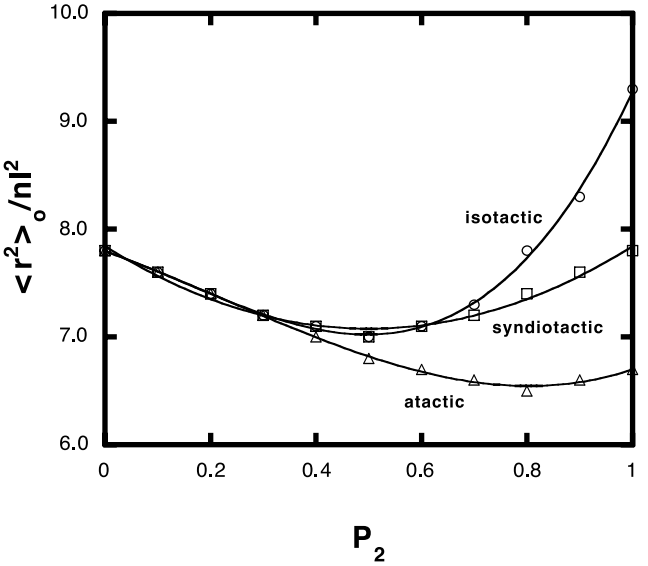

Fig. 9. Characteristic ratio, $C_n = \langle r^2 \rangle_0 / nl^2$, of isotactic, syndiotactic and atactic ethylene–propylene copolymers as a function of the probability of occurrence of the propylene units in the chain microstructure, P_2.

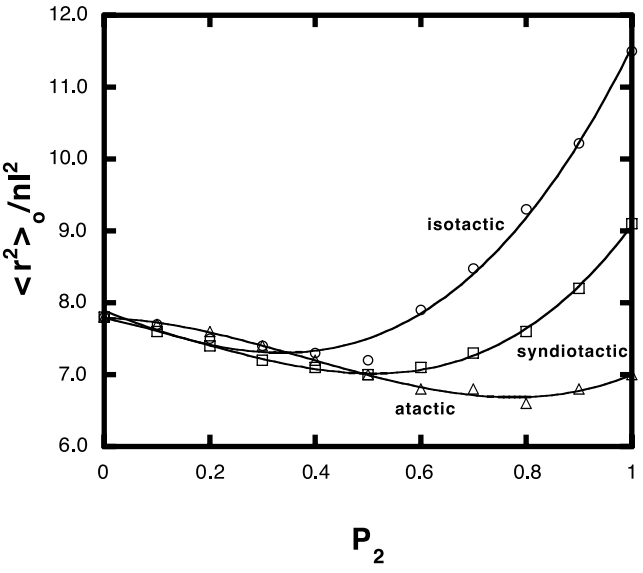

Fig. 10. Characteristic ratio, $C_n = \langle r^2 \rangle_0 / nl^2$, of isotactic, syndiotactic and atactic ethylene-1-butene copolymers as a function of the probability of occurrence of the 1-butene units in the chain microstructure.

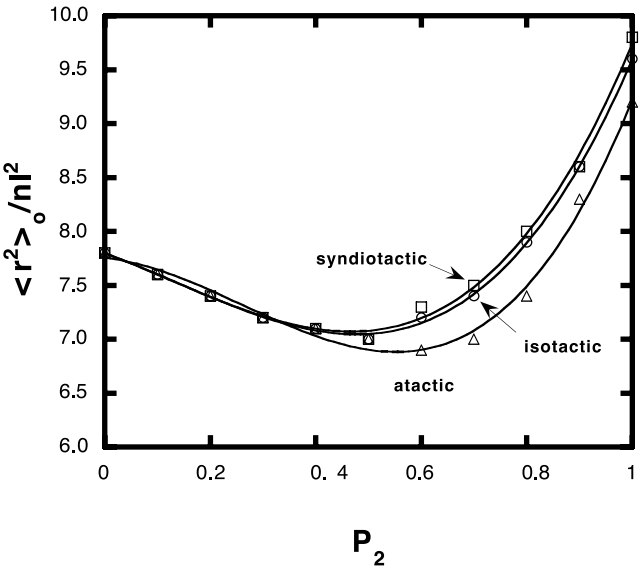

Fig. 12. Characteristic ratio, $C_n = \langle r^2 \rangle_0 / nl^2$, of isotactic, syndiotactic and atactic ethylene-1-octene copolymers as a function of the probability of occurrence of the 1-octene units in the chain microstructure.

function of P_2, the probability of occurrence of 1-olefin units in the chain microstructure. For the three different stereochemical structures, each entry is the average calculated from 20,000 generated microstructures meeting the criteria cited above as well as the conformational validation of the statistical weight factors. This is done by continuously comparing the probabilities calculated from the RIS procedures with those resulting from molecular dynamics simulations in accordance with the method of Mattice et al. [32].

The figures show that, in all cases, the characteristic ratios of the various homopolymers decrease upon the addition of units of the other comonomer. In case of copolymer chains

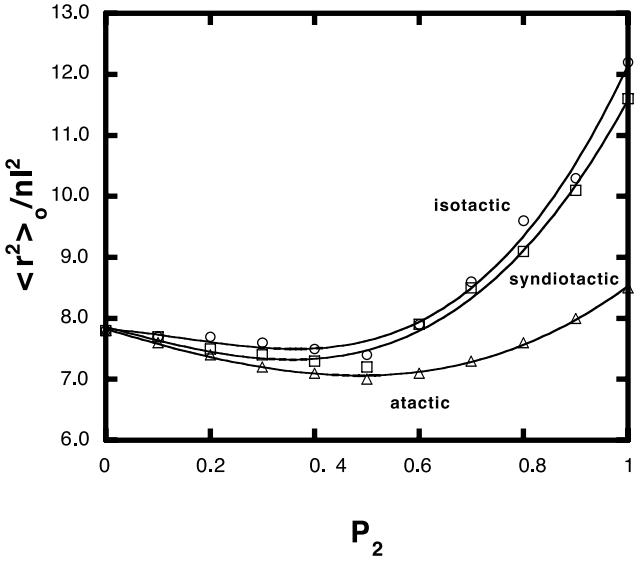

Fig. 11. Characteristic ratio, $C_n = \langle r^2 \rangle_0 / nl^2$, of isotactic, syndiotactic and atactic ethylene-1-hexene copolymers as a function of the probability of occurrence of the 1-hexene units in the chain microstructure.

that contain predominantly ethylene units, the 1-olefin units cause departures from the extended all-*trans* conformations, which are the low energy forms for ethylene sequences. For chains consisting mostly of highly isotactic 1-olefin units, the ethylene units disrupt the low energy conformations of the extended helical sequences, causing a decrease in their characteristic ratios as was also observed by Mark for ethylene–propylene copolymers [27]. Similar influences were also observed for the syndiotactic copolymeric microstructures but to a lesser extent than that of the isotactic case. Interestingly, however, the addition of the ethylene units to a chain predominantly rich in atactic placements had little effect on the characteristic ratio of the 1-olefin sequences. This observation is consistent with earlier observations that atactic homopolymers have abnormally low characteristic ratios [27,40]. There is one exception, however, to this observation, which is the case of atactic ethylene–octene copolymer, Fig. 12. The behavior of the atactic copolymer, in this case, is closely related to the behavior of the isotactic and syndiotactic ones. As indicated earlier from the probability distribution surfaces, the long side chains of the octene comonomer units hinders the formation of extended regular conformations, giving rise to lower values for the unperturbed dimensions of the regular stereochemical structures. This will result in bringing the overall values for the characteristic ratios of the isotactic and syndiotactic ethylene–octene copolymers close to those of the atactic ones. The decrease in the characteristic ratio of the copolymers with the increase in the comonomer content indicates that the articulated side group leads, via non-bonded interactions, to an enhancement, in terms of the three rotational states, of the *gauche* conformer population in the main backbone.

By performing further molecular dynamics simulations

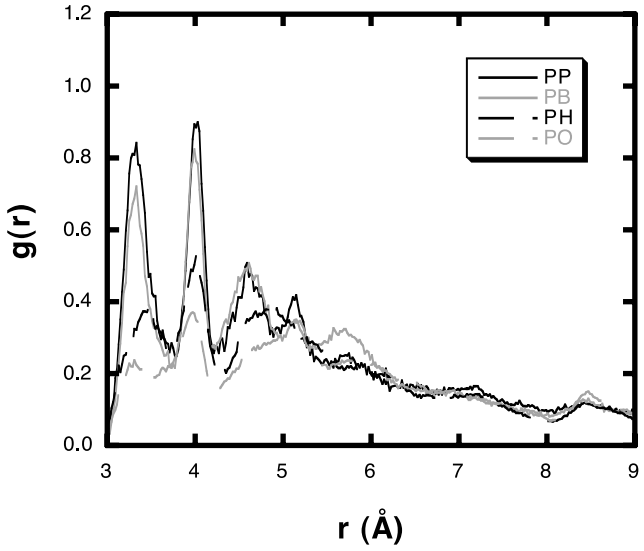

Fig. 13. The radial distribution function of isotactic PP, PB, PH, and PO calculated at 473 K.

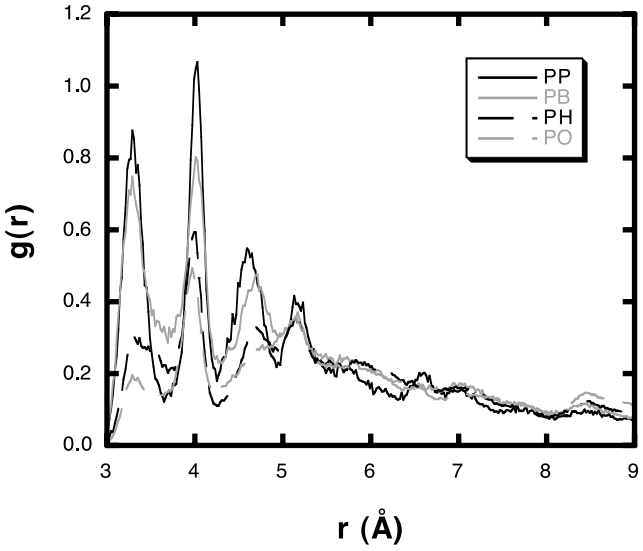

Fig. 15. The radial distribution function of atactic PP, PB, PH, and PO calculated at 473 K.

[26,39,42,45] of the various copolymeric structures of 200 units at 473 K using NPT ensembles for 100 ps for equilibration at the relative densities of the ensembles followed by another 100 ps using NVT ensembles and applying the periodic boundary conditions, the radial distribution function, $g_{\alpha\beta}(r)$, is calculated from the average of the static relationship of every given pair of particles, αβ, as

$$g_{\alpha\beta}(r) = \frac{\langle n_{\alpha\beta}(r)\rangle}{4\Pi r^2 \Delta r \rho_{\alpha\beta}} \tag{15}$$

where $\langle n_{\alpha\beta}(r)\rangle$ is the average number of atom pairs in the spherical shell between r and $r + \Delta r$, and $\rho_{\alpha\beta}$ is the density of atom pairs of type αβ. The radial distribution functions are used to characterize the local packing and the intermolecular structure of the melts. In this investigation, $g(r)$ is evaluated for all pairs of carbon atoms in different chains and all pairs of carbon atoms in the same chain that are separated by at least four bonds [46]. The radial distribution functions for all the homopolymers, obtained as the average over the whole molecular dynamics trajectories are depicted in Fig. 13–15 for the isotactic, syndiotactic and atactic homopolymers, respectively. The figures show that the minima and maxima for the various polymers occur at the same position regardless its stereochemical composition. The amplitudes, however, of these peaks may differ according to the polymeric chemical and stereochemical structures. The longer the side chains the lower the amplitude of the various peaks, which indicates denser packing and an increased pair correlation at longer distances. The effect of tacticity [47] on the local packing of PB chains is greatly pronounced. The maxima and minima in case of PB is more sharply defined in the isotactic case than in the syndiotactic and atactic cases in agreement with observations made earlier from the probability distribution surfaces. Such an effect is not observed in case of PO chains, which indicates the increased level of disorder in these chains, possibly due to the increase in the methyl–methyl interactions in the side chains on the expense of the backbone–backbone interactions. The increased level of disorder in the local packing of PO chains could be obvious from the lack of influence of the tacticity of the PO chains on its dihedral angle pair correlation as was also indicated from the probability distribution surfaces, Figs. 3–5.

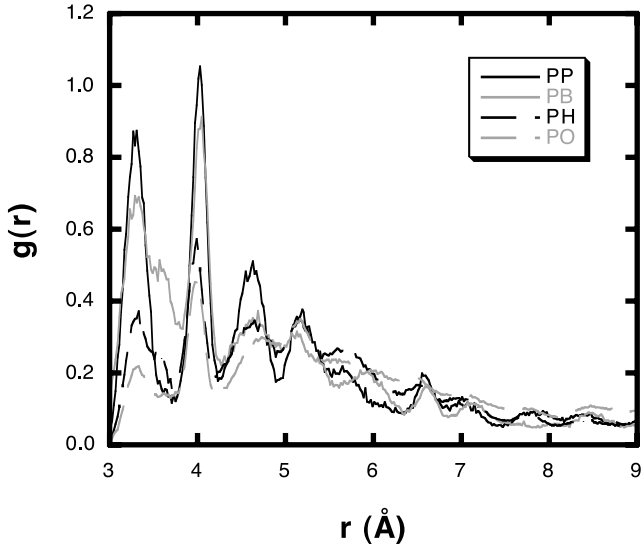

Fig. 14. The radial distribution function of syndiotactic PP, PB, PH, and PO calculated at 473 K.

4. Conclusion

Molecular dynamics techniques can be employed in order to simulate realistically the role of chain microstructure of

ethylene-1-olefin copolymers on its conformational behavior in direct relation to the interesting experimental observations of this class of polymers. However, in order to sample all of the conformational space of sufficiently long polymer chains using the time-consuming molecular dynamics techniques, very long dynamics runs would be needed. The use of well-known methods such as the rotational isomeric state approximation may provide a better approach for the simulation of the conformational behavior of the polymeric chain using reasonable resources. The statistical weights of the statistical weight matrices commonly employed in this approach can be evaluated by the integration of the molecular dynamics trajectories of sufficient length for the various oligomers. These statistical weight matrices can be used further to evaluate the conditional probabilities, which may be used in conjunction with Monte Carlo methods to simulate, realistically, various conformations of the different polymeric microstructures. The probability distribution surfaces of the various homopolymers were constructed by evaluating the probability of occurrence of a joint state for a pair of bonds over the whole conformational space. It is obvious from these probability distribution surfaces that the increased length of the side chains has increased the probability of the $g^{\pm}t$ joint states at the expense of $g^{\pm}g^{\pm}$ pairs leading naturally to an apparent extension of the polymeric chains. Interestingly, this behavior had a maximum at poly(1-butene)/poly(1-hexene) accompanied by a decrease in the characteristic ratio of the homopolymers with the increase in the side chain length such as the case of poly(1-octene). Similar observations were also obtained for the syndiotactic case. This behavior was explained by considering the increased frequency for potential overlaps between the long side chains giving rise to third- and higher-order interactions. These side chains mutually exclude each other from otherwise accessible space and the longer the side chain is, the more relevant this space exclusion must be. At such a point, when the side chains are long enough and much more excluded space is therefore necessary, the main backbone chain may have to coil onto itself to allow for the longer side chains to point outwards, giving rise to much lower values for the unperturbed end-to-end distance and subsequently lower values for the characteristic ratio. Interestingly, in case of isotactic poly(1-octene), the main backbone of the polymer chain may favor the *gauche*$^{+}$ and *gauche*$^{-}$ dihedral states in order to accommodate the side chain crowding resulting from the placement of the long side chains at the same side of the main backbone, whereas in case of syndiotactic poly(1-octene), the main backbone will favor more the *trans* torsional angle in order to accommodate the long substituents placed opposite each other along the main backbone.

Adding 1-olefin units to ethylene sequences in the case of ethylene-1-olefin copolymers caused departures for the ethylene sequences from the extended all-*trans* conformations. For chains consisting mostly of highly isotactic or highly syndiotactic 1-olefin units, the ethylene units disrupted the low energy conformations of the extended helical sequences and thus caused a decrease in their characteristic ratios. Addition of the ethylene units to a chain predominantly rich in atactic placements had little effect on the characteristic ratio of the 1-olefin sequences in agreement with results obtained from the probability distribution sequences. The effect of tacticity on the local packing of 1-olefin chains as observed from the radial distribution function of the various homopolymers showed that the maxima and minima in the case of poly(1-butene) are more sharply defined in the isotactic case than in the syndiotactic and atactic cases.

Acknowledgements

TM and BG are indebted to KULeuven for supporting their visiting scholar and postdoctoral positions. HR is grateful to FWO-Vlaanderen for a research grant.

References

[1] Mathot VBF. In: Mathot VBF, editor. The crystallization and melting region in calorimetry and thermal analysis of polymers. Munich: Hanser, 1994. p. 231, chapter 9.
[2] Vanden Eynde S, Rastogi S, Mathot VBF, Reynaers H. Macromolecules 2000;33:9696.
[3] Mathot VBF, Fabrie CCM. J Polym Sci, Polym Phys Ed 1990;28:2487.
[4] Mathot VBF, Fabrie CCM, Tiemersmathoone GPJM, van der Velden GPM. J Polym Sci, Polym Phys Ed 1990;28:2509.
[5] Hoffman JD, Davis GT, Lauritzen JI. In: Happay NB, editor. Treatise on solid state chemistry, vol. 3. New York: Plenum Press, 1976. p. 497.
[6] Hoffman JD, Miller RL, Marand H, Roitman DB. Macromolecules 1992;25:2221.
[7] Tashiro K, Sasaki S, Gose N, Kobayashi M. Polym J 1998;30:485.
[8] Rastogi S, Hikosaka M, Kawabata H, Keller A. Macromolecules 1991;24:6384.
[9] Okada T, Saito H, Inoue T. Macromolecules 1992;25:1908.
[10] Bates FS, Fredrickson GH. Macromolecules 1994;27:1065.
[11] Fredrickson GH, Liu AJ, Bates FS. Macromolecules 1994;27:2503.
[12] Fredrickson GH, Liu AJ. J Polym Sci, Polym Phys Ed 1995;33:1203.
[13] Crist B, Hill MJ. J Polym Sci, Polym Phys Ed 1997;35:2329.
[14] Mandelkern L. In: Mark JE, editor. Physical properties of polymers, 2nd ed. Washington, DC: American Chemical Society, 1993.
[15] Ward IM. Mechanical properties of solid polymers. 2nd ed. New York: Wiley, 1983.
[16] Sun T, Brant P, Chance RR, Graessley WW. Macromolecules 2001;34:6812.
[17] Scholte TG, Meijerink NLJ, Schoffeleers HM, Brands AMG. J Polym Sci, Polym Phys Ed 1984;29:3763.
[18] Flory PJ. Statistical mechanics of chain molecules. New York: Wiley, 1969.
[19] Flory PJ. Br Polym J 1976;8:1.
[20] Flory PJ. Macromolecules 1974;7:381.
[21] Volkenstein MV. Configurational statistics of polymeric chains. New York: Interscience Publishers, 1963.
[22] Birshtein TM, Ptitsyn OB. Conformations of macromolecules. New York: Interscience Publishers, 1966.
[23] Flory PJ, Ciferri A, Chiang R. J Am Chem Soc 1961;83:1023.

[24] Roovers J, Martin JE. J Polym Sci, Polym Phys Ed 1989;27:2513.
[25] Roovers J. Polymer 1985;26:1091.
[26] Madkour TM, Ibrahim OM, Ebaid AH. J Macromol Sci, Phys 2000;39:679.
[27] Mark JE. J Chem Phys 1972;57:2541.
[28] Mattice WL. Macromolecules 1977;10:1171.
[29] Flory PJ, Mark JE, Abe A. J Am Chem Soc 1966;88:639.
[30] Mattice WL, Suter UW. Conformational theory of large molecules. New York: Wiley, 1994.
[31] Wittwer H, Suter UW. Macromolecules 1985;18:403.
[32] Neuburger N, Bahar I, Mattice WL. Macromolecules 1992;25: 2447.
[33] Bahar I, Zuniga I, Dodge R, Mattice WL. Macromolecules 1991;24:2986.
[34] Zuniga I, Bahar I, Dodge R, Mattice WL. J Chem Phys 1991;95:5348.
[35] Mattice WL, Dodge R, Zuniga I, Bahar I. Comput Polym Sci 1991;1:35.
[36] Madkour TM, Mark JE. Comput Polym Sci 1994;4:79.
[37] Madkour TM, Mark JE. Macromolecules 1995;28:6865.
[38] Abe A, Jernigen RL, Flory PJ. J Am Chem Soc 1966;88:631.
[39] Madkour TM, Ibrahim OM, Ebaid AH. Comput Polym Sci 2000;10:15.
[40] Abe A. Polym J 1970;1:232.
[41] Lee S, Sun H, Kim B, Freed KF. J Chem Phys 2001;114:5537.
[42] Madkour TM. Angew Makromol Chem 1999;266:63.
[43] Cho D, Neuburger NA, Mattice WL. Macromolecules 1992;25:322.
[44] Lee K-J, Mattice WL. Comput Polym Sci 1991;1:213.
[45] Madkour TM, Mohamed S, Barakat AM. Polymer 2002;43:533.
[46] Akten ED, Mattice WL. Macromolecules 2001;34:3389.
[47] Madkour TM, Soldera A. Eur Polym J 2001;37:1105.
[48] Brandrup J, Immergut EH. Polymer handbook. 3rd ed. New York: Wiley, 1989.
[49] Alamo RG, Mandelkern L. Thermochim Acta 1994;238:155.